Letter

Light-driven Lifshitz transitions in non-Hermitian multi-Weyl semimetals

Debashree Chowdhury,[1,*] Ayan Banerjee,[2,†] and Awadhesh Narayan[2,‡]
[1]*Centre of Nanotechnology, Indian Institute of Technology Roorkee, Roorkee, Uttarakhand-247667, India*
[2]*Solid State and Structural Chemistry Unit, Indian Institute of Science, Bangalore 560012, India*

(Received 8 December 2020; revised 23 April 2021; accepted 27 April 2021; published 19 May 2021)

Non-Hermitian topological systems are the newest additions to the growing field of topological matter. In this work, we report the light-driven exceptional physics in a multi-Weyl semimetal. The driving is not only a key ingredient to control the position of the exceptional contours (ECs); light also has the ability to generate new ECs. Interestingly, we also demonstrate topological charge distribution and Lifshitz transition, which are controllable by the driving field in such generated ECs. Our findings present a promising platform for the manipulation and control over exceptional physics in non-Hermitian topological matter.

DOI: 10.1103/PhysRevA.103.L051101

Topology plays a pivotal role in the study of condensed matter systems, with wide focus on topological insulators and superconductors in the last decade [1–3]. The new feather in the cap is the study of topological semimetals (TSMs) [4], among which Weyl semimetals (WSMs) [5] have attracted a great recent interest. In contrast to a topological insulator, WSMs are gapless in the bulk and break either or both time reversal and inversion symmetries. The WSM spectra is linear near Weyl points, which usually come in pairs and act as sources and sinks of the Berry curvature with monopole charge ± 1. Furthermore, WSMs with quadratic, cubic, or even higher order dispersion have also been proposed [6–10]. These are coined as double, triple, or, in general, multi-WSMs. Besides having a nonlinear dispersion relation, these WSMs are unique in the sense that they are protected by rotation symmetries of different point groups [11], specifically the n-fold rotation symmetry C_n [6–11] and they have integer topological charges greater than unity.

In the last few years, the analysis of non-Hermitian (NH) gain and loss terms on different topological properties have captivated the research community [12–22]. Many experimental efforts have strengthened the theoretical predictions in systems such as ultracold atoms [23,24] and optics [25,26]. An unconventional feature that makes these systems special is their defectiveness, i.e., merging of eigenstates at some particular points, where the eigenenergies also coalesce [27]. These special degenerate points are called exceptional points (EPs) [27–30]. In addition to having a single EP, there may also arise exceptional surfaces with a collection of EPs, termed exceptional contours (ECs) in a multidimensional parameter space [13,29,31].

Tuning properties of quantum systems with light has been a promising new frontier in recent years [32–48]. Interaction with topology has led to unveiling of numerous exciting phenomena; for instance, in conventional TSMs the light induces new phases [33] and can cause profound changes in the Fermi surface topology, which is coined as the Lifshitz transition [49–53]. On the other hand, in linear WSMs circularly polarized light (CPL) can cause a tuning of the distance between the two Weyl points resulting in an anomalous Hall effect [54,55].

In this Letter, we have analyzed the ECs that appear in NH multi-WSMs in the presence of CPL. We show that the driving can be used as a facile tool to generate ECs [56–60]. In addition, besides controlling the position of the exceptional rings one can also generate new ECs. Furthermore, we study the charge division of the newly created ECs by means of NH generalization of the Berry curvature, and the concomitant Lifshitz transitions. In Fig. 1, we present a schematic for the Lifshitz transition of a double Weyl semimetal and the generation of new ECs in the presence of both CPL and gain or loss parameters. Importantly, one can notice that the exceptional ring, which appears due to the gain or loss term in the absence of light (left panel in Fig. 1), divides into two exceptional rings when light is switched on.

We start with the analysis of effects of driving on the band structure of NH multi-WSMs. The low energy Hamiltonian of an n-th order multi-WSM in the presence of the NH loss or gain term is [29]

$$H^{\eta,n}(q) = \frac{1}{2m}(q_-^n\sigma_+ + q_+^n\sigma_-) + (\eta v_z q_z + i\zeta)\sigma_z, \quad (1)$$

where ζ is the gain or loss parameter. Here $q_\pm = q_x \pm iq_y$ and $\sigma_\pm = \sigma_x \pm i\sigma_y$, with σ_i and q_i $(i = x, y, z)$ denoting the components of Pauli matrices and quasimomentum, respectively. Here, m is the quasiparticle mass, $\eta = \pm 1$, and v_z is the z component of the Fermi velocity. The corresponding energy eigenvalues are in general complex. This complex spectra of the system causes some accidental degeneracies, where not only the eigenenergies coalesce, but also eigenvectors merge; these degeneracy points are coined as EPs. Our aim is to find out the exact positions of these EPs and the effect of these degeneracies on different physical properties. In the case of a

*debashreephys@gmail.com
†ayanbanerjee@iisc.ac.in
‡awadhesh@iisc.ac.in

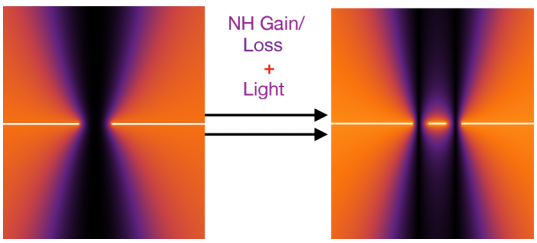

FIG. 1. Schematic of proposal for light-induced Lifshitz transition in a double Weyl semimetal. A combination of NH terms and driving converts a single exceptional ring into two exceptional rings.

usual WSM, it is shown in the previous work [28] that adding a NH term to the Hamiltonian can convert the Weyl point into an exceptional ring, which carries the same charge as that of the original Weyl point [29]. Furthermore, depending on the strength of the gain or loss term, it is also possible to merge two ECs of opposite charge and in the process of this merging, they annihilate and form a single contour [29].

In order to investigate the physical properties of such a NH system under driving, let us include an optical field polarized in the x-z plane of the form $\mathcal{E}(t) = \mathcal{E}_0(\cos\Omega t, 0, -\sin\Omega t)$, where $\mathcal{E}_0$ and Ω are the amplitude and frequency of the driving optical field. The minimal substitution leads to $\hbar q_i \to \hbar q_i + eA_i$, where e is the electronic charge, A is the vector potential with $\vec{A}(t+T) = \vec{A}(t)$, and $T = 2\pi/\Omega$ is the periodicity. Floquet theory is an elegant method to incorporate the periodic driving effects on the band structure. In Floquet formalism we consider a time dependent periodic Hamiltonian $H(t+T) = H(t)$ that exhibits quasiperiodic eigenspectra. Interestingly, non-Hermitian Floquet systems admit complex quasienergies with some periodicity leading to a point gap topology with nontrivial winding associated with quantized charge transport, which has no analog in conventional Hermitian physics [61]. Although Floquet theory is valid for all frequency regimes of the driving field, here we restrict ourselves to the high frequency (HF) regime, where the frequency of the optical field is much larger than the bandwidth of the system. This HF approximation has similarities with the rotating wave approximation. This eventually breaks the time reversal symmetry (TRS), and as a result a gap opening can be observed in several systems. Importantly, in charge ± 1 WSMs the gap opening at the Weyl point is not possible with this HF laser light. Rather the optical field leads to a shift of the Weyl points of the TRS broken WSMs. For multi-WSMs, we find a rather interesting role of light in the presence of loss or gain terms. In the HF approximation, it is possible to easily calculate the effective time independent Hamiltonian using the Floquet-Magnus expansion [19,32,33,37]. Thus we have [11]

$$H^{n,\eta}_{\rm eff}(q) = \frac{1}{2m}\big[\big(q_-^n + i\Delta q_-^{n-1}\big)\sigma_+ + \big(q_+^n - i\Delta q_+^{n-1}\big)\sigma_-\big] + (\eta v_z q_z + i\zeta)\sigma_z, \quad (2)$$

where $\Delta = \frac{nA_0^2 v_z \eta}{2\hbar\Omega}$, where A_0 and Ω are the amplitude and frequency of the driving field, respectively.

The corresponding energy eigenvalues are

$$\mathcal{E}_{m,\pm} = \pm\sqrt{\frac{\big(q_x^2+q_y^2\big)^{(n-1)}\big[q_x^2+(q_y-\Delta)^2\big]}{m^2} - (\zeta - iq_z v_z \eta)^2}. \quad (3)$$

The band diagrams with topological charge $n = 2$ and $n = 3$ are shown in Fig. 2. In general, from Eq. (3), we find the nth-order polynomial, $f(q)$, governing the locations of the EPs as

$$f(q) = q_{\rm EP_n}^{2n} - 2\Delta q_{\rm EP_n}^{2n-1} + \Delta^2 q_{\rm EP_n}^{2n-2} - m^2\zeta^2 = 0. \quad (4)$$

Using Descartes's sign rule, we find a maximum of three positive real roots and one negative real root. All other roots are imaginary. Thus by tuning the relative strength of the light intensity and the gain and loss parameters, the positions of these four roots can be manipulated. Two or three EPs can be superimposed by adjusting the two parameters. Notably, the condition to achieve the superimposition of l number of EPs is $f^i(q_{\rm EP}) = 0$ for $i = 0, 1, \ldots, l$. Thus, for $n = 2$, one observes that the two EPs sit together for $\Delta = 2\sqrt{\zeta}$. The general criterion for finding the ECs in NH systems is $\mathcal{E}_{m,+} = \mathcal{E}_{m,-}$, which is equivalent to

$$\begin{aligned} &\mathrm{Re}\,\det[H^{\eta,n}(q)] = 0, \\ &\mathrm{Im}\,\det[H^{\eta,n}(q)] = 0. \end{aligned} \quad (5)$$

These two constraint equations (in three-dimensional systems) allow higher-dimensional surfaces to form but are restricted to exhibit only one-dimensional ECs [29]. Along these one-dimensional contours, the eigenvalues coalesce and the eigenvectors also merge.

Let us now discuss the specific cases of double ($n = 2$) and triple ($n = 3$) WSMs in more detail. In the case of the double WSM the Floquet effective Hamiltonian can be written as $H^{\eta}_{\rm eff}(q) = \mathbf{d}(q)\cdot\boldsymbol{\sigma}$, where $\boldsymbol{d} = \mathbf{d}_R + i\mathbf{d}_I$ with $\mathbf{d}_R, \mathbf{d}_I \in \Re^3$ and $\boldsymbol{\sigma}$ the vector of standard Pauli matrices. Using Eq. (5) one obtains the locations of EPs as follows:

$$q_{\rm EP} = \Delta/2 \pm \sqrt{\Delta^2/4 \pm \zeta}, \quad (6)$$

where we have chosen $\phi = \pi/2$.

As a consequence of the quadratic dependence of momentum in Eq. (3) for $n = 2$, in general we get four EPs in the $q_z = 0$ plane. The position of the EPs can be further tuned by varying the light intensity as we present in Fig. 3. Depending upon the strength of the light field and the NH term, one obtains two EPs when the momentum coordinates of the other two EPs become imaginary, and three EPs when two EPs coincide with each other for a particular value of light intensity, i.e., $\Delta = 2\sqrt{\zeta}$.

We present the fate of ECs in the presence of light in Fig. 4 and interestingly, we find that light accomplishes topological charge division by splitting the parent contour symmetrically or asymmetrically, as we will discuss next. For double WSMs, one observes that the single contour is divided into two symmetric contours with the increase of the driving amplitude [Figs. 4(a)–4(c)]. In Fig. 4(d), we show a similar analysis for a triple WSM. Unlike the double WSM case, where the parent contour is divided into two

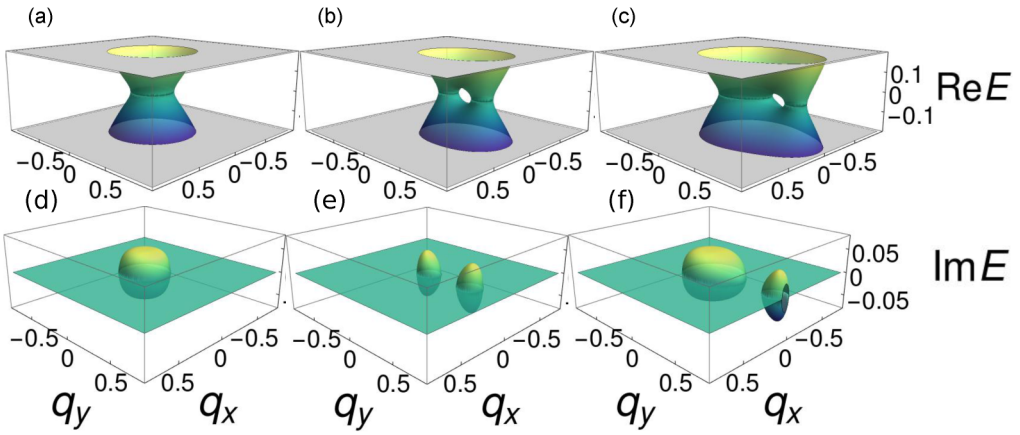

FIG. 2. Band diagrams showing Lifshitz transitions for multi-WSM. The real and imaginary parts of the dispersion for double WSM ($n = 2$) [(a) and (d)] in the absence of light, and [(b) and (e)] with $A_0 = 0.77$ and $\zeta = 0.08$. (c) and (f) The real and imaginary parts of the dispersion for triple WSM ($n = 3$) in the presence of light with $A_0 = 0.7$ and $\zeta = 0.04$. In the absence of light one has a single exceptional ring (ER) for $n = 2$ and $n = 3$. With increasing light intensity the single ring turns into two ERs resulting in Lifshitz transitions. Here we set $\Omega = 1.0$, $q_z = 0.0$, $\eta = 1.0$, and $v_z = 1.0$.

symmetric contours, in triple WSMs the division is asymmetric. This is due to the fact that driving divides the ECs into those corresponding to a double Weyl and a linear Weyl.

An important question next arises: how does the value of the topological charge in the newly generated ECs depend on the driving field? To answer this question, we consider the non-Hermitian generalization of the Berry charge [62] as $\mathfrak{N} = \int_C \mathbf{\Omega}^{LR}(\mathbf{k}) \cdot d\mathbf{S}$, where $\mathbf{\Omega}^{LR}(\mathbf{k})$ is the Berry curvature which can be obtained as $\nabla \times \mathcal{A}^{LR}(\mathbf{k})$, with $\mathcal{A}^{LR}(\mathbf{k})$ being the Berry gauge field [11]. $\mathcal{A}^{LR}$ is obtained from the left and right eigenvectors ($\psi^{L/R}$) of the Hamiltonian as $\mathcal{A}^{LR}(k) = i\langle\psi^L(k)|\nabla|\psi^R(k)\rangle$.

We note that it is shown in Ref. [28] that after integrating the Berry curvature on a closed surface, which encloses the ECs, the Berry charge is real and quantized. Here we have shown that in the presence of the driving field, the charge solely depends on the driving amplitude and when the amplitude crosses a limiting value the charge division occurs. In Fig. 5, the plot of Berry curvature density for the double WSM is presented. One observes that when light amplitude is less than 0.8, we obtain only one divergence in the Berry curvature density distribution; this is the region where the topological charge accumulates. An increase of the driving amplitude causes the $\mathbf{\Omega}^{LR}(\mathbf{k})$ to show discontinuity at two different places, which in turn denotes the accumulation of charges at two different places and results in the division of the ECs. A similar argument can be drawn for the multi-WSM case as well [11].

We map out the topological phase diagram next, by computing the vorticity of constitutive bands. One can define the vorticity, ν_{mn}, for any pair of bands (E_m and E_n) with complex

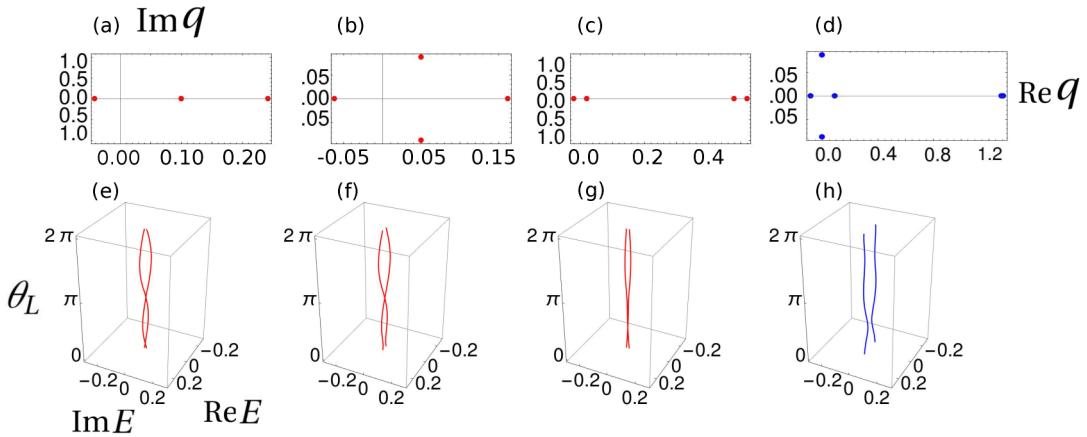

FIG. 3. Locations of exceptional points and analysis of vorticity. The locations of (a)–(c) four exceptional points for $n = 2$ and (d) eight exceptional points for $n = 3$ for different light intensities. Corresponding vorticity plots are shown in the lower panel. (e) The vorticity of two bands encircling two exceptional points sitting together with the same winding number for $A_0 = 0.447$ [corresponding to (a)]. Vorticity plots for (f) $A_0 = 0.32$ and (g) $A_0 = 0.7$ encircling the leftmost EP and third EP corresponding to (b) and (c), respectively. (h) The vorticity plot for $n = 3$ with $A_0 = 0.9$ encircling two EPs with the same position and opposite winding numbers showing the absence of swapping. Here we set $\zeta = 0.01$.

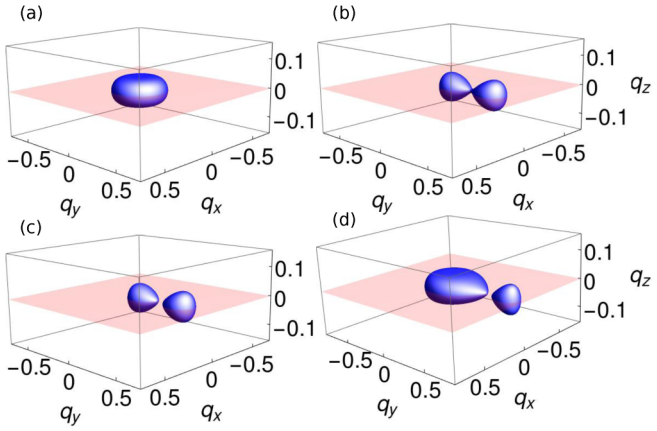

FIG. 4. Light-tunable exceptional contours for non-Hermitian multi-Weyl semimetals. The real (blue) and imaginary (orange) exceptional surfaces are shown, and their intersection defines the ECs. ECs for double WSMs ($n = 2$) (a) in the absence of light, (b) at critical light intensity with $A_0 = 0.66$, and (c) at a higher light intensity $A_0 = 0.68$. (d) EC for $n = 3$ is shown for light amplitude $A_0 = 0.68$. We clearly see the evolution of contours with increasing light intensity, showing topological charge division arising from Lifshitz transitions. Here we set $\zeta = 0.05$.

energy dispersion as [63]

$$\nu_{mn}(\Gamma) = -\frac{1}{2\pi}\oint_{\Gamma} \nabla_{\mathbf{k}} \arg[E_m(\mathbf{k}) - E_n(\mathbf{k})]\, d\mathbf{k}, \tag{7}$$

where Γ is a closed loop encircling the EP in the momentum space. The energy eigenvalue for a single complex band of NH Hamiltonian in general can be written as $E(\mathbf{k}) = |E(\mathbf{k})|e^{i\theta_L(k)}$, where $\theta_L = \tan^{-1}(\mathrm{Im}E/\mathrm{Re}E)$. Fractional vorticity is an inherent property of the EPs and is well defined in the absence of any symmetry [63]. We present the vorticity and its tuning by light for our WSM systems in Figs. 3(e)–3(h). When the chosen contour encircles an odd number of EPs, the two bands swap with each other in the complex plane owing to the square root singularity, and the vorticity takes a half-integer value. On the other hand, when an even number of EPs are enclosed, the vorticity becomes an integer [64].

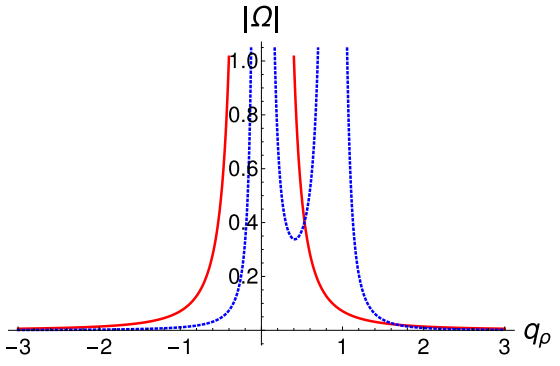

FIG. 5. Berry curvature density tuning with light. Normalized Berry curvature density as a function of the radial momentum without light (red solid) and with $A_0 = 0.8$ and $\zeta = 0.05$ (blue dashed). The divergences signal the presence of band degeneracy where the topological charge accumulates. In the absence of light we obtain a single peak, while beyond the critical light intensity the two peaks confirm the charge division. Here $q_x = q_\rho \cos\phi$ and $q_y = q_\rho \sin\phi$. We further choose $\phi = \pi/2$.

A complementary diagnostic of the NH topological bands is the winding number, W_N. By considering q_x, q_y, and q_z as parameters one can define it as [14,65]

$$W_N = \frac{1}{2\pi}\int_{-\infty}^{\infty} dk_z \partial_{k_z}\phi_{xz}, \tag{8}$$

where $\phi_{xz} = \arctan(\frac{h_x}{h_z})$. Here h_x and h_z are the components of the Hamiltonian and can be found by comparing Eq. (2) (for $n = 2$) with $H = h_x\sigma_x + h_z\sigma_z$. We find the general expressions for the winding number for multi-WSMs. Depending on whether n is even or odd, different values of the winding number are obtained. The winding number in the $k_x = 0$ plane is obtained as [11]

$$W_N = \frac{\mathrm{Sgn}(\mathcal{B}^n + m\zeta) + \mathrm{Sgn}(\mathcal{B}^n - m\zeta)}{4}, \tag{9}$$

where

$$\mathcal{B}^n = -\Delta k_y^{n-1} + k_y^n, \qquad n = 1, 2, 3 \ldots. \tag{10}$$

We find a clear dependence of the winding number on the light-induced term. For $n = 1, 3, 5\ldots$ the winding number has values as $\pm 1/2$ for contours enclosing EPs and zero otherwise. On the contrary, for $n = 2, 4, 6\ldots$ the values are $1/2$ for contours which enclose the EP and 0 otherwise. This further confirms the control over EPs with driving.

Finally, let us discuss the experimental feasibility of our work. During the last few years, experimental efforts to investigate the role of NH loss and gain on different topological properties in systems such as dissipative waveguides and cold-atom platforms [24,28,66–68] were initiated, where the generation of EPs has been analyzed [67,69]. In Ref. [28], the creation of ECs was experimentally demonstrated in helical waveguides, where the existence of Weyl points was observed. The inclusion of some cuts in the waveguides gives rise to the NH term, which in turn produces the ECs, and their real and quantized topological charge has also been measured [28]. To observe these ECs, in [29], the authors use metallic chiral woodpile photonic crystals, where Weyl points with topological charges 1 and 2 can be found by introducing complex on-site energy [70]. On the other hand, in cold-atom systems [23] the NH and driving aspects are incorporated through atomic population control [71] and shaking of an optical lattice [72]. Another important direction to experimentally realize our results is to consider a topoelectrical circuit [73–75] for multi-WSMs. We have presented a circuit diagram of such a circuit for realization of double WSMs [11]. In this setup it is possible to realize the circuit parameters in terms of the Hamiltonian of the double WSMs. The experimental detection of nodal band structures is possible by capturing the complex admittance spectra for each fixed q_y, and striking changes can be observed in complex admittance spectra at q_{EP}, which enables the detection of the ERs and changes in the Fermi surface. Here the Floquet term could easily be incorporated by switching on and off the circuit abruptly. It is important to note that the circuit elements can be reliably time modulated through the use of metal-oxide-semiconductor field-effect

transistors that allow component parameters, i.e., inductance, to be switched via external control voltages.

In summary, we have explored the role of driving with light in NH multi-WSMs. We have illustrated our proposal of how driving allows control over existing ECs, as well as enables spawning new ECs. This is one of the main highlights of our work. We have further pointed out that light allows tuning of distribution of topological charge as well as Lifshitz transitions. The charge division is demonstrated through the analysis of the NH generalization of the Berry curvature, which shows a single discontinuity when the light amplitude is less than a critical value. Upon increasing the light amplitude, one comes across a discontinuity of the Berry curvature at two different values of the momentum: this signals a splitting of the EC and a division of the topological charge. Furthermore, we have diagnosed the exceptional physics by means of vorticity and winding number computations. We hope our results motivate future theoretical and experimental investigations of the interplay between driving and non-Hermiticity.

D.C. acknowledges financial support from DST (Project No. SR/WOS-A/PM-52/2019). A.B. would like to acknowledge the Prime Ministers Research Fellowship. A.N. acknowledges support from a startup grant (Grant No. SG/MHRD-19-0001) of the Indian Institute of Science and DST-SERB (Project No. SRG/2020/000153).

[1] M. Z. Hasan and C. L. Kane, Rev. Mod. Phys. **82**, 3045 (2010).
[2] O. Vafek and A. Vishwanath, Annu. Rev. Condens. Matter Phys. **5**, 83 (2014).
[3] C. L. Kane and E. J. Mele, Phys. Rev. Lett. **95**, 226801 (2005).
[4] A. A. Burkov, Nat. Mater. **15**, 1145 (2016).
[5] N. P. Armitage, E. J. Mele, and A. Vishwanath, Rev. Mod. Phys. **90**, 015001 (2018).
[6] C. Fang, M. J. Gilbert, X. Dai, and B. A. Bernevig, Phys. Rev. Lett. **108**, 266802 (2012).
[7] G. Xu, H. Weng, Z. Wang, X. Dai, and Z. Fang, Phys. Rev. Lett. **107**, 186806 (2011).
[8] S.-M. Huang, S.-Y. Xu, I. Belopolski, C.-C. Lee, G. Chang, T.-R. Chang, B. Wang, N. Alidoust, G. Bian, M. Neupane, D. Sanchez, H. Zheng, H.-T. Jeng, A. Bansil, T. Neupert, H. Lin, and M. Zahid Hasan, Proc. Natl. Acad. Sci. USA **113**, 1180 (2016).
[9] S.-X. Zhang, S.-K. Jian, and H. Yao, Phys. Rev. B **96**, 241111(R) (2017).
[10] A. Gupta, arXiv:1703.07271.
[11] See Supplemental Material at http://link.aps.org/supplemental/10.1103/PhysRevA.103.L051101 for a detailed discussion on Floquet high frequency approximation, symmetries of multi-Weyl semimetals, Berry curvature analysis, computational details of winding number, and the topoelectric circuits for double Weyl semimetals.
[12] A. Ghatak and T. Das, J. Phys.: Condens. Matter **31**, 263001 (2019).
[13] E. J. Bergholtz, J. C. Budich, and F. K. Kunst, Rev. Mod. Phys. **93**, 015005 (2021).
[14] Z. Gong, Y. Ashida, K. Kawabata, K. Takasan, S. Higashikawa, and M. Ueda, Phys. Rev. X **8**, 031079 (2018).
[15] P. St-Jean, V. Goblot, E. Galopin, A. Lemaître, T. Ozawa, L. Le Gratiet, I. Sagnes, J. Bloch, and A. Amo, Nat. Photonics **11**, 651 (2017).
[16] M. A. Bandres, S. Wittek, G. Harari, M. Parto, J. Ren, M. Segev, D. N. Christodoulides, and M. Khajavikhan, Science **359**, eaar4005 (2018).
[17] L. Zhou and J. Gong, Phys. Rev. B **98**, 205417 (2018).
[18] T. E. Lee, Phys. Rev. Lett. **116**, 133903 (2016).
[19] P. He and Z.-H. Huang, Phys. Rev. A **102**, 062201 (2020).
[20] L. Zhou, Phys. Rev. B **101**, 014306 (2020).
[21] S. Jana, D. Chowdhury, and A. Saha, arXiv:2010.02852.
[22] D. Leykam, K. Y. Bliokh, C. Huang, Y. D. Chong, and F. Nori, Phys. Rev. Lett. **118**, 040401 (2017).
[23] N. Goldman, J. C. Budich, and P. Zoller, Nat. Phys. **12**, 639 (2016).
[24] Y. Xu, S.-T. Wang, and L.-M. Duan, Phys. Rev. Lett. **118**, 045701 (2017).
[25] J. Noh, W. A. Benalcazar, S. Huang, M. J. Collins, K. P. Chen, T. L. Hughes, and M. C. Rechtsman, Nat. Photonics **12**, 408 (2018).
[26] R. El-Ganainy, M. Khajavikhan, D. N. Christodoulides, and S. K. Ozdemir, Commun. Phys. **2**, 37 (2019).
[27] L. E. F. Foa Torres, J. Phys.: Mater. **3**, 1 (2019).
[28] A. Cerjan, S. Huang, M. Wang, K. P. Chen, Y. Chong, and M. C. Rechtsman, Nat. Photonics **13**, 623 (2019).
[29] A. Cerjan, M. Xiao, L. Yuan, and S. Fan, Phys. Rev. B **97**, 075128 (2018).
[30] E. J. Bergholtz and J. C. Budich, Phys. Rev. Res. **1**, 012003(R) (2019).
[31] A. Cerjan, A. Raman, and S. Fan, Phys. Rev. Lett. **116**, 203902 (2016).
[32] T. Oka and H. Aoki, Phys. Rev. B **79**, 081406(R) (2009).
[33] J. Cayssol, B. Dóra, F. Simon, and R. Moessner, Phys. Status Solidi RRL **7**, 101 (2013).
[34] N. H. Lindner, G. Refael, and V. Galitski, Nat. Phys. **7**, 490 (2011).
[35] M. C. Rechtsman, J. M. Zeuner, Y. Plotnik, Y. Lumer, D. Podolsky, F. Dreisow, S. Nolte, M. Segev, and A. Szameit, Nature (London) **496**, 196 (2013).
[36] Y. Wang, H. Steinberg, P. Jarillo-Herrero, and N. Gedik, Science **342**, 453 (2013).
[37] M. S. Rudner and N. H. Lindner, Nat. Rev. Phys. **2**, 229 (2020).
[38] A. Narayan, Phys. Rev. B **91**, 205445 (2015).
[39] Z. Yan and Z. Wang, Phys. Rev. Lett. **117**, 087402 (2016).
[40] C. K. Chan, Y. T. Oh, J. H. Han, and P. A. Lee, Phys. Rev. B **94**, 121106(R) (2016).
[41] A. Narayan, Phys. Rev. B **94**, 041409(R) (2016).
[42] K. Taguchi, D. H. Xu, A. Yamakage, and K. T. Law, Phys. Rev. B **94**, 155206 (2016).
[43] Z. Yan and Z. Wang, Phys. Rev. B **96**, 041206(R) (2017).
[44] R. Jaiswal and A. Narayan, Phys. Rev. B **102**, 245416 (2020).
[45] J. W. McIver, B. Schulte, F.-U. Stein, T. Matsuyama, G. Jotzu, G. Meier, and A. Cavalleri, Nat. Phys. **16**, 38 (2020).

[46] S. A. Sato, J. W. McIver, M. Nuske, P. Tang, G. Jotzu, B. Schulte, H. Hübener, U. De Giovannini, L. Mathey, M. A. Sentef, A. Cavalleri, and A. Rubio, Phys. Rev. B **99**, 214302 (2019).
[47] H. Hübener, M. A. Sentef, U. De Giovannini, A. F. Kemper, and A. Rubio, Nat. Commun. **8**, 13940 (2017).
[48] E. J. Sie, C. M. Nyby, C. D. Pemmaraju, S. Ji Park, X. Shen, J. Yang, M. C. Hoffmann, B. K. Ofori-Okai, R. Li, A. H. Reid, S. Weathersby, E. Mannebach, N. Finney, D. Rhodes, D. Chenet, A. Antony, L. Balicas, J. Hone, T. P. Devereaux, T. F. Heinz, X. Wang, and A. M. Lindenberg Nature (London) **565**, 61 (2019).
[49] R. J. Kirby, L. Muechler, S. Klemenz, C. Weinberg, A. Ferrenti, M. Oudah, D. Fausti, G. D. Scholes, and L. M. Schoop, arXiv:2011.04646.
[50] H. F. Yang, L. X. Yang, Z. K. Liu, Y. Sun, C. Chen, H. Peng, M. Schmidt, D. Prabhakaran, B. A. Bernevig, C. Felser, B. H. Yan and Y. L. Chen, Nat. Commun. **10**, 3478 (2019).
[51] J. Y. Lin, N. C. Hu, Y. J. Chen, C. H. Lee, and X. Zhang, Phys. Rev. B **96**, 075438 (2017).
[52] G. E. Volovik, Low Temp. Phys. **43**, 47 (2017).
[53] S. Beaulieu, S. Dong, N. Tancogne-Dejean, M. Dendzik, T. Pincelli, J. Maklar, R. Patrick Xian, M. A. Sentef, M. Wolf, A. Rubio, L. Rettig, and R. Ernstorfer, arXiv:2003.04059.
[54] R. Chen, B. Zhou, and D.-H. Xu, Phys. Rev. B **97**, 155152 (2018).
[55] C.-K. Chan, P. A. Lee, K. S. Burch, J. H. Han, and Y. Ran, Phys. Rev. Lett. **116**, 026805 (2016).
[56] L. Zhou and J. Pan, Phys. Rev. A **100**, 053608 (2019).
[57] L. Zhou, Phys. Rev. B **100**, 184314 (2019).
[58] J. Pan and L. Zhou, Phys. Rev. B **102**, 094305 (2020).
[59] L. Zhou, Y. Gu, and J. Gong, Phys. Rev. B **103**, L041404 (2021).
[60] A. Banerjee and A. Narayan, J. Phys.: Condens. Matter **33**, 225401, (2021).
[61] B. Höckendorf, A. Alvermann, and H. Fehske, Phys. Rev. Res. **2**, 023235 (2020).
[62] M. R. Hirsbrunner, T. M. Philip, and M. J. Gilbert, Phys. Rev. B **100**, 081104(R) (2019).
[63] H. Shen, Bo Zhen, and L. Fu, Phys. Rev. Lett. **120**, 146402 (2018).
[64] A. Banerjee and A. Narayan, Phys. Rev. B **102**, 205423 (2020).
[65] C. Yin, H. Jiang, L. Li, R. Lü, and S. Chen, Phys. Rev. A **97**, 052115 (2018).
[66] B. Midya, H. Zhao, and L. Feng, Nat. Commun. **9**, 1 (2018).
[67] C. Dembowski, H.-D. Gräf, H. L. Harney, A. Heine, W. D. Heiss, H. Rehfeld, and A. Richter, Phys. Rev. Lett. **86**, 787 (2001).
[68] V. M. Alvarez, J. B. Vargas, M. Berdakin, and L. F. Torres, Eur. Phys. J.: Spec. Top. **227**, 1295 (2018).
[69] K. Ding, G. Ma, M. Xiao, Z. Q. Zhang, and C. T. Chan, Phys. Rev. X **6**, 021007 (2016).
[70] M.-L. Chang, M. Xiao, W.-J. Chen, and C. T. Chan, Phys. Rev. B **95**, 125136 (2017).
[71] L. Li, C. H. Lee, and J. Gong, Phys. Rev. Lett. **124**, 250402 (2020).
[72] G. Jotzu, M. Messer, R. Desbuquois, M. Lebrat, T. Uehlinger, D. Greif, and T. Esslinger, Nature (London) **515**, 237 (2014).
[73] X.-X. Zhang and M. Franz, Phys. Rev. Lett. **124**, 046401 (2020).
[74] C. H. Lee, S. Imhof, C. Berger, F. Bayer, J. Brehm, L. W. Molenkamp, T. Kiessling, and R. Thomale, Commun. Phys. **1**, 39 (2018).
[75] J. Dong, V. Juricic, and B. Roy, Phys. Rev. Res. **3**, 023056 (2021).